Journal Pre-proof

KRIT1 as a possible new player in melanoma aggressiveness

Jasmine Ercoli, Federica Finetti, Brittany Woodby, Giuseppe Belmonte, Clelia Miracco, Giuseppe Valacchi, Lorenza Trabalzini

PII: S0003-9861(20)30492-6

DOI: https://doi.org/10.1016/j.abb.2020.108483

Reference: YABBI 108483

To appear in: *Archives of Biochemistry and Biophysics*

Received Date: 3 February 2020

Revised Date: 30 June 2020

Accepted Date: 2 July 2020

Please cite this article as: J. Ercoli, F. Finetti, B. Woodby, G. Belmonte, C. Miracco, G. Valacchi, L. Trabalzini, KRIT1 as a possible new player in melanoma aggressiveness, *Archives of Biochemistry and Biophysics* (2020), doi: https://doi.org/10.1016/j.abb.2020.108483.

Ercoli Jasmine, performed major part of the experiments, methodology, roles/writing – original draft

Finetti Federica, conceptualization, supervision, roles/writing-original draft

Woodby Britney, conceptualization, supervision, roles/writing-original draft

Belmonte Giuseppe, data curation, investigation, methodology

Miracco Clelia, data curation, investigation, methodology

Valacchi Giuseppe, conceptualization, funding acquisition, supervision, writing – review & editing

Trabalzini Lorenza, conceptualization, funding acquisition, supervision, writing – review & editing

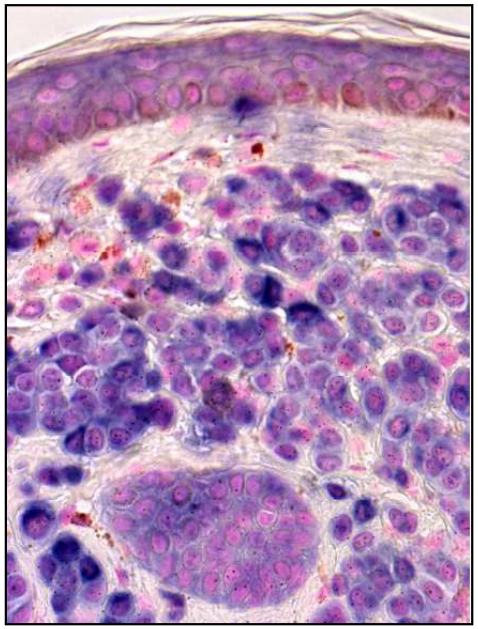

KRIT1 - Benign nevus

KRIT1 loss

Transformation

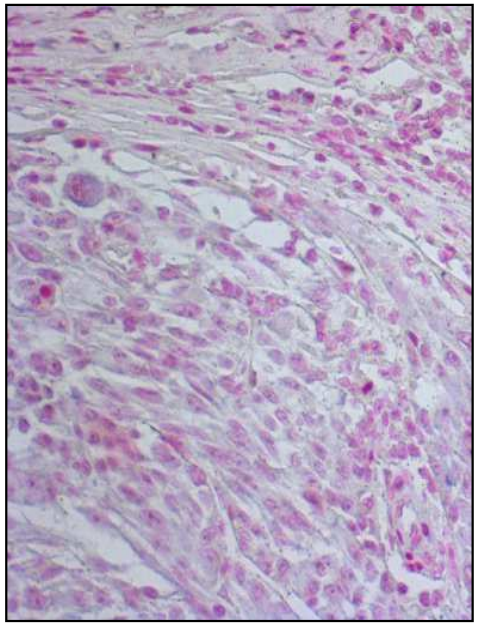

KRIT1 - Melanoma

↓ proliferation
↓ migration and invasion
↓ mesenchymal markers
↓ inflammation

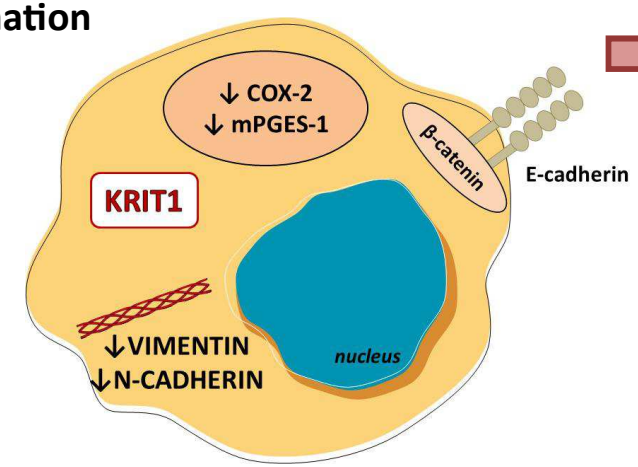

Melanocyte

↑ proliferation
↑ migration and invasion
↑ mesenchymal markers
↑ inflammation

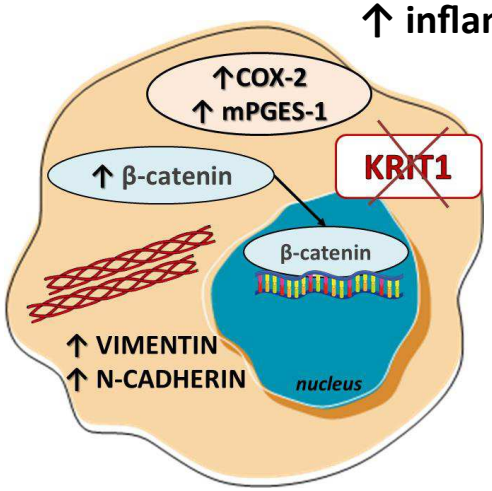

Melanoma cell

KRIT1 as a possible new player in melanoma aggressiveness

Jasmine Ercoli[1], Federica Finetti[1], Brittany Woodby[2], Giuseppe Belmonte[3], Clelia Miracco[3], Giuseppe Valacchi[2,4,5§], Lorenza Trabalzini[1§]

[1] Department of Biotechnology, Chemistry and Pharmacy, University of Siena, Italy

[2] Plants for Human Health Institute, NC Research Campus, NC State University, NC, USA;

[3]Unit of Pathological Anatomy, Department of Medicine, Surgery, and Neurosciences, University of Siena, Siena, Italy

[4]Dept. of Biomedical and Specialist Surgical Sciences, University of Ferrara, Ferrara, Italy;

[5]Department of Food and Nutrition, Kyung Hee University, Seoul, South Korea.

[§] These authors equally contributed to the work

Corresponding authors:

e-mail addresses:

lorenza.trabalzini@unisi.it (L. Trabalzini)

gvalacc@ncsu.edu (G. Valacchi)

ABSTRACT:

Krev interaction trapped protein 1 (KRIT1) is a scaffold protein known to form functional complexes with distinct proteins, including Malcavernin, PDCD10, Rap1 and others. It appears involved in several cellular signaling pathways and exerts a protective role against inflammation and oxidative stress. KRIT1 has been studied as a regulator of endothelial cell functions and represents a determinant in the pathogenesis of Cerebral Cavernous Malformation (CCM), a cerebrovascular disease characterized by the formation of clusters of abnormally dilated and leaky blood capillaries, which predispose to seizures, neurological deficits and intracerebral hemorrhage. Although KRIT1 is ubiquitously expressed, few studies have described its involvement in pathologies other than CCM including cancer. Cutaneous melanoma represents the most fatal skin cancer due to its high metastatic propensity. Despite the numerous efforts made to define the signaling pathways activated during melanoma progression, the molecular mechanisms at the basis of melanoma growth, phenotype plasticity and resistance to therapies are still under investigation.

The hypothesis driving this work is that KRIT1 may control melanoma progression by acting as a tumor suppressor. Here, we show that KRIT1 is expressed in normal human melanocyte but is lacking in melanoma. In human cell model of melanoma KRIT1 silencing induced increased growth and invasion and a switch toward a malignant cell phenotype. These data candidate KRIT1 as a new possible player of a complex signalling network that regulates melanoma progression and offer a new possible target for melanoma therapies.

Keywords

KRIT1, melanoma, tumor suppressor, N-cadherin, inflammation, β-catenin.

1. INTRODUCTION:

KRIT1 (Krev interaction trapped protein-1) is an intracellular protein isolated by a two-hybrid screening through its interaction with the Ras-family GTPase Krev1/Rap1a [1]. KRIT1 lacks defined catalytic domains while contains a well characterized protein-protein interaction motifs and domains, including three NPXY/F motifs, three ankyrin repeats and a FERM domain. It has been extensively described that KRIT1 is able to form functional complexes with distinct proteins, comprising Malcavernin (CCM2), PDCD10 (CCM3), ICAP1, Rap1, Nd1-L and others [2–6].

KRIT1 is ubiquitously expressed during early embryogenesis, followed by a restricted expression which persists up to adult life. During this second phase, KRIT1 is mainly expressed in neuronal cells of central and peripheral nervous system and in various epithelia (epidermal, digestive, respiratory, uterine and urinary) both in mouse and human [7].

KRIT1 signalling pathway has been extensively studied since its mutation causes Cerebral Cavernous Malformations (CCMs), a rare vascular disease typically found in the central nervous system with a prevalence of 0.3%-0.5% of the population [8,9]. CCMs are characterized by thin walled vessels lacking of normal structure [10–12]. In the CCM disease, endothelial cells of brain vessels acquire characteristics comparable to tumors including increased growth and migration, reduced apoptosis, endothelial mesenchymal transition, loss of cell-cell junction, pro-inflammatory status, altered redox homeostasis and activation of growth factors receptor signalling.

The mechanisms by which the loss of KRIT1 leads to vascular malformations has not yet been fully clarified, although many evidences support pleiotropic effects related to the eventual ability of KRIT1 to modulate several mechanisms involved in angiogenesis, vascular homeostasis, cell responses to oxidative stress and inflammation, including cytoskeleton dynamics [2,13–19]. KRIT1 is associated with microtubules, membranes, adherents junctions and cellular nucleus [20]. In particular, as Rap1 GTPase effector, KRIT1 interacts with cell junctions in a complex with VE-cadherin, p120-catenin and β-catenin [5]. Consequently, KRIT1 depletion could induce the loss of a stable cellular architecture and the activation of TGFβ/BMP signalling downstream of β-catenin [21].

Previous studies demonstrated that KRIT1 is an antiangiogenic protein able to keep the human endothelium quiescent and to inhibit proliferation, migration, lumen formation and sprouting angiogenesis [17,22–24]. In addition, KRIT1 negatively coordinates cell cycle by controlling FoxO-mediated downregulation of cyclin D1 and upregulation of p27Kip1 levels through the modulation of intracellular reactive oxygen species (ROS) levels [25].

Based on its ability to regulate several signaling pathways and its ubiquitous expression, KRIT1 is likely to be involved in others pathological conditions than CCM. To date, very few studies have demonstrated that KRIT1 is implicated in other pathologies as cardiovascular disease [26], diabetes [16], intestinal epithelial barrier dysregulation [14] and cancer [27,28]. In particular, the involvement of KRIT1 as tumor suppressor in cancer has been hypothesized since the oncogenic miR-21 expression anticorrelates with KRIT1 [27]. No other data are available in the literature on the contribution of KRIT1 in cancer progression.

Cutaneous malignant melanoma (CMM), which comprises 5% of all skin cancers, is the most aggressive and highly lethal form of skin cancer [29,30]. Several factors contribute to the formation of melanoma, including exposure to ultraviolet (UV) radiation and the malignant transformation of nevus, along with a variety of genetic factors [31]. Most forms of melanoma are sporadic, so the somatic mutations are acquired during person's lifetime and are present only in the melanocytes that give rise to the melanoma. In some cases this is the result of environmental insults followed by proto-oncogene activation coupled with suppression of tumor suppressor genes and defects in DNA repair mechanism [32]. The malignancy is more likely to spread in patients with deep primary tumors or regional lymph node metastases, which leads to a median survival of only 6–9 months [33]. Significant progress has been made in the identification of genetic markers and cellular pathways involved with the melanoma progression to identify novel therapeutic targets; nevertheless, additional key players underlying melanoma onset and progression need to be identified. Recently, mutations of genes involved in human melanoma have also been found in angiomas [34,35].

Taken together, all these elements gave rise to the idea that KRIT1 could be involved in the onset and progression of melanoma. To demonstrate that we investigated the role of KRIT1 in the growth and metastasis of melanoma by using KRIT1 knockdown melanoma cells and specimens from patients. We hypothesized that KRIT1 may play an important role in the formation of melanoma metastasis and may control tumor progression by acting as a suppressor. This novel hypothesis opens the avenue to the study of a completely new role of KRIT1 in cancer development giving new perspectives for melanoma prevention and treatment.

2. MATERIALS AND METHODS:

2.1 Cell culture

A375 melanoma cells (ATCC, Rockville, MD, USA) were cultured in DMEM (Gibco, Waltham, MA, USA) supplemented with 10% fetal bovine serum (FBS, Hyclone, Chicago, IL, USA), 100 U/ml penicillin/streptomycin (Gibco), and 4 mM L-glutamine (Corning, NY, USA) [36].

2.2 Human melanocytic samples analysis

Taking advantage of the rich collection of samples kept at the Section of Pathological Anatomy of the Azienda Ospedaliera Universitaria Senese (Siena, Italy), we choose 57 consecutive samples of melanocytic lesions with a 5-year minimum follow up (see Tab1). They included 5 benign common nevi (BCN); 5 dysplastic nevi (DN); 5 radial growth phase melanomas (RGPMM), 23 vertical growth phase malignant melanomas (VGPMM) and 11 melanoma metastases (MelMet). As inclusion criteria, we chose frozen samples with mutations for BRAF, NRAS, and C-KIT. Control samples were represented by healthy skin from the lesion margins.

2.3 Immunohistochemistry

As previously described [37], tissue slides were deparaffinised in xylene and dehydrated in ethanol. Microwave pre-treatment in 10 mM citrate buffer (pH 6.0) was performed for 30 min. Non-specific binding was blocked for 20 min with 2.5% normal horse serum (NHS). The slides were incubated with primary antibodies targeting KRIT1 (1:100; ThermoFisher, Waltham, MA, USA) followed by chromogenic visualization using ImmPress-AP (Vector). In particular, sections were incubated for 15 min with NBT-BCIP added with Levamisole. After counterstaining with nuclear fast red (NFR), slides were washed thoroughly, dehydrated, cleared in xylene and mounted. Staining intensity was scored as negative (no staining) or positive (blue colour). Fluorescence quantification was calculated as ratio between the area of each cell and the fluorescence intensity.

A semiquantitative evaluation of the immunostaining was performed by using the software ImageJ (version 1.52v, https://imagej.nih.gov/ij/). KRIT1-immunostained cytoplasm of normal melanocytes served to choose the threshold. All tumor sections were examined.

2.4 siRNA transfection

A375 cells, were plated (5.0×10^5 cells/well) on 6 well multiplates and after adhesion transfected with 50 nM of control or KRIT1 siRNA (Qiagen, Hilden, Germania) using 4 µL of lipofectamine

3000 (Invitrogen, Carlsbad, CA, USA), according to manufacturer's instructions and as previously described [38]. 6 hours post-transfection, cells were washed with PBS, and media was changed. Cells were used for experiments 24 hours post-transfection.

2.5 MTT assay

Cells were plated (2.0 x 10^4 cells/well) in 96 wells multiplates in DMEM 10% FBS. After 24 hrs, the medium was removed, and cells were incubated for 4 hours with fresh medium in the presence of 1.2 mM MTT (3-(4,5-dimethylthiazol-2-yl)-2,5-diphenyltetrazolium bromide) (Sigma-Aldrich,St. Louis, MO, USA). The MTT solution was removed and 100 µL of DMSO were added to each well to dissolve the blue formazan crystals. The absorbance of the formazan dye was measured at 570 nm with a microplate reader (Spectramax M5 multimode microplate reader, Molecolar Device, San Jose, CA, USA). Data were expressed as a percentage of the basal control [39].

2.6 BrdU assay

For 5-bromo-2-deoxyuridine (BrdU) experiments, A375 cells were seeded (5.0 x 10^3 cells/well) in a 96-well plate and incubated overnight. The next day, cells were transfected with 50nM concentration of either control or KRIT1 siRNA using 0.3 uL of lipofectamine 3000 in 200 uL total volume of media, using the same method as previously mentioned (see siRNA transfection section for method). Six hours post-transfection, medium was changed. BrdU experiments were performed 24 hours post-transfection, using a BrdU assay kit (Roche, catalog no. 11 647 229 001), and BrdU was added to the cells for 1 hour (as suggested by the manufacturer for this cell line). After labeling, cell culture medium was removed. Next, the cells were fixed, and the DNA was denatured by adding FixDenat (from kit). Then, anti-BrdU-POD, an anti-BrdU antibody conjugated with peroxidase, was added to the samples. This antibody binds to newly, synthesized cellular DNA with BrdU incorporated. Next, the cells were washed with PBS, and the peroxidase substrate was added. Absorbance was measured at λ 370 nm (reference wavelength: 492 nm). [38]

2.7 Migration assay

A375 cells were seeded (1.0 x 10^6 cells/well) in 24-well multiplate in DMEM 10% FBS. After 12 hours, cell monolayers were scored vertically down the center of each well with a sterile tip. Each well was washed with PBS to remove detached cells. Fresh medium (1% serum), with ARA C (Sigma–Aldrich) (2.5 mg/ml) to inhibit cell proliferation, was added. Images of the wound in each well were acquired at time 0 and after 6 and 12 hours (magnification of 10X). Results were

expressed as arbitrary units of wound and percentage of healing taking as reference the area at time 0 [39].

2.8 Invasion assay

Chemotaxis experiments were performed using trans-well system. The day before, the trans-well was coated with gelatin 0.25% (100 µL /well) and maintained overnight at 4°C. A375 cells were plated (1.0 x 10^5 cell/well) in coated trans-well in DMEM without FBS, and 650 µL of DMEM 10% FBS were added in the lower chamber. The cells were incubated and after 12, 18 and 24 hours were fixed in EtOH 70%, colored with Coomassie Blue solution (10% Acetic acid, 10% ethanol and 0,25% Blue Coomassie) and washed with DDI water.

The number of migrated cells present in five fields/well was counted at 20X magnification. Data were reported as percentage of migrated cells [41]

2.9 Protein extraction and Western blotting

Cells silenced with siKRIT1 and siCTRL were seeded at the density of 500,000 cells/well in 6 well multiplates in DMEM with 10% FBS. After 24 hours, cells were lysated and briefly centrifuged at 15,000×g for 20 min at 4 °C.

Protein content was measured using a BCA protein assay kit (Thermo Scientific). For Western blotting analysis, aliquots of cell extract supernatants containing an equal amount of proteins (50 µg) were treated with Laemmli buffer, boiled for 10 min, resolved on 4-20% stain-free gel and then blotted onto a nitrocellulose membrane. Membranes were incubated with 1:1,000 dilutions of anti-KRIT1 (Millipore, Burlington, MA, USA), anti-β actin (Sigma Aldrich), anti-β-catenin (Santa Cruz, Dallas, TX, USA), anti-vimentin (Santa Cruz), anti-N-cadherin (Bioss, Woburn, MA, USA), anti-COX-2 (Cell signaling, Danvers, MA, USA), anti-mPGES-1 (Santa Cruz) or anti-cyclin D1 (BioRad, Hercules, CA, USA) antibody. The membranes were then incubated with 1:10,000 dilutions of horseradish peroxidase-conjugated secondary antibody (BioRad) for 1 hour at RT. Chemiluminescence was detected by ChemiDoc imager (BioRad), and quantification was performed using Image J [43].

2.10 MMP activation assay

5 x 10^4 cells/well (A375) were cultured in 96-well cell culture plates in 10% fetal bovine serum medium. After adhesion, cells were incubated with 50 µL of serum-free conditioned media. After 48 hours, media were collected, clarified by centrifugation and assayed by zymography. Media were subjected to electrophoresis in 8% SDS-PAGE containing 1 mg/ml gelatin under non-

denaturing conditions, by using Sample Buffer w/o β-ME and sample boiling. After electrophoresis, gel were washed with 2.5% Triton X-100 to remove SDS and incubated for 48 hours at 37°C in 50 mM Tris buffer containing 200 mM NaCl and 20 mM CaCl2, pH 7.4. Gels were stained with 0.05% Coomassie brilliant blue R-250 in 10% acetic acid and 10% ethanol and destained with 10% acetic acid and 10% ethanol. Bands of gelatinase activity appeared as transparent areas against a blue background. Gelatinase activity was then evaluated by quantitative densitometry [15,42].

2.11 Proliferation assay

A375 cells were seeded in 96-well microplates (2.0 x 10^4 cells/well) in DMEM 10% FBS and after 12 and 18 and hours they were fixed for 10 min with 70% EtOH and colored with Coomassie Blue solution (10% Acetic acid, 10% ethanol, and 0,25% Blue Coomassie).

The number of proliferated cells present in five fields/well was counted at 20X magnification. Data were reported as percentage of proliferating cells [40].

2.12 Immunofluorescence analysis

A375 cells (2.5 x 10^5 cells/well) were seeded on glass cover-slips. After 24 hours cells were fixed with formalin for 10 min and permeabilized with PBS 0.25% Triton x100 for 10 min, incubated with 1% BSA for 30 min and stained overnight at 4 °C with primary antibody for β-catenin, Vimentin and N-cadherin (Santa Cruz). Slips were washed three times with PBS and then incubated 1 hour at room temperature with Alexa Fluor 568 or 488 secondary antibodies (ThermoFisher Scientific, Waltham, MA, USA). Nuclei were stained with 1 μg/ml DAPI (D1306 Invitrogen, USA) for 1 min after removal of secondary antibody. Microscopy imaging was performed on Olympus IX71/X51 (Olympus Life science) inverted microscope using a 60X objective [43].

The Corrected Total Cell Fluorescence (CTCF) was measured in at least 15 view fields at 600X magnification. The images were taken at the same exposition time and light intensity. Then, the data were evaluated using the ImageJ software measuring total cell area and a region next to selected cell as background. The following equation was used:

CTCF = integrated density − (area of selected cell × mean fluorescence of background readings)

To study β-catenin cellular localization, the intensity of nuclear and cytoplasmic fluorescence was measured in siCTRL and siKRIT1 cells and the following formula was applied: siCTRL([intensity in the cytoplasm] / [intensity in the nucleus]) versus siKRIT1([intensity in the cytoplasm] / [intensity in the nucleus]).

2.13 Statistical analysis

Data were generated from three independent experiments and expressed as means ± standard deviation (SD). Statistical analysis was performed using Student's t test for unpaired data; $p<0.05$ was considered statistically significant.

3 RESULTS:

3.1 KRIT1 expression in benign melanocytes and in melanoma

In the adult life the expression levels of KRIT1 are higher in endothelium and in neuronal cells of central and peripheral nervous system but it is known that KRIT1 is also present in endothelia [44] and in various epithelia such as epidermal, digestive, respiratory, uterine and urinary [7]. Although, several studies have been performed in order to define the physio-pathological role of KRIT1 in Cerebral Cavernous Malformation models, very few studies report the involvement of KRIT1 in other pathologies. To explore a possible role of KRIT1 in cancer, and in particular in melanoma progression, in this study we evaluated the expression levels of KRIT1 by immunohistochemical and Western blot analysis in human specimens (Fig.1A). In all sections, the endothelium was intensely positive to KRIT1, and it represented our internal positive control. KRIT1 immunopositivity was also observed in the luminal side of the sweat glands epithelium. Normal melanocytes, as well as benign common nevi (BCN), were strongly decorated by KRIT1 (Fig. 1A, panel a). In dysplastic nevi (DN) and in radial growth phase melanomas (RGPM), single melanocytes and groups of negative melanocytes were observed, disorderly mixed with positive melanocytes. The quantification of immunohistochemical images shows a significant and progressive decrease of KRIT1 protein expression in DN, vertical growth phase melanomas (VGPM), and melanoma metastasis (MelMet), when compared to BCN, with the lowest values registered in MelMet. In addition, these data were confirmed by Western blot analysis of the corresponding frozen samples (Fig 1B). These data indicated a possible regulatory role of KRIT1 in melanoma metastasis.

3.2 KRIT1 knockdown stimulates cellular proliferation in A375 cells

In order to investigate the role of KRIT1 in melanoma progression, we knocked down KRIT1 in A375 cells using siRNA transfection (siKRIT1 A375) (Fig. 2A). We observed that KRIT1 knockdown increased cellular viability measured by MTT assay **(**Fig. 2B**)** and, consistently, stimulated cellular proliferation (Fig. 2C and D). Furthermore, we observed increased in cyclin D1 and decrease in p27 levels in siKRIT1 A375 cells respect to siCTRL A375 cells (Fig. 2E).

3.3 KRIT1 downregulation increases migration and invasion in A375 melanoma cells

In view of the observation reported for human melanoma samples, we evaluated whether loss of KRIT1 affected cell migration and invasion by using a wound closure *in vitro* scratch assay. As reported in Fig. 3A, the rate of wound closure in siKRIT1 A375 cells was faster than in siCTRL A375 cells. Additionally, we performed a migratory assay to assess whether knockdown of KRIT1

affected the ability of the cells to directionally move towards a selected chemoattractant. We observed that knockdown of KRIT1 promoted cell invasion (Fig. 3B**)**. It is known that the invasion process is linked to activation of metalloproteinases (MMPs), key enzymes involved in extracellular matrix (ECM) degradation and in the regulation of cancer cells invasion into surrounding tissue/circulation [45]. In addition, the ability of KRIT1to affect MMP2 activity was also assessed and as shown in Fig.3C, silencing KRIT1 increased MMP-2 activity in melanoma cells.

3.4 KRIT1 knockdown induces β-catenin nuclear translocation and the expression of metastatic markers of A375 melanoma cells

Since we observed increased migration and invasion in siKRIT1 cells, we hypothesized that knockdown of KRIT1 may affect also phenotype plasticity through regulation of the Wnt/β-catenin signalling pathway [46]. Perturbations in Wnt□β□catenin signalling and elevated β□catenin levels are positively correlated with melanoma aggressiveness and are associated with melanoma malignant phenotype [47]. In addition, it has been already demonstrated that knockdown of KRIT1 increases nuclear β-catenin localization and activation of β-catenin-dependent transcription [24].

As shown in Fig. 4A, siKRIT1 A375 cells showed higher levels of β-catenin expression in respect to siCTRL cells. Moreover, immunofluorescence analysis of β-catenin localization indicated a shift of the protein from cytoplasm to nucleus (Fig. 4B).

As nuclear translocation of β-catenin leads to transcription of β-catenin genes [48], which are involved in EMT associated protein network and in melanoma plasticity, we measured the levels of EMT proteins as vimentin and N-cadherin in siKRIT1 and siCTRL A375 cells [49]. As shown in Fig. 5, silencing KRIT1 increased the levels of both mesenchymal markers, evaluated by both, Western blot (Fig. 5A) and immunofluorescence (Fig. 5B).

Recently it has been reported that melanoma progression and metastatization is linked to inflammatory pathways [50–53]. In addition, elevated expression of cyclooxigenase-2 (COX-2) plays an important role in tumorigenesis as mediating the progression and metastasis of many epithelial cancer and melanoma [54]. As reported in Fig. 6 siKRIT1 A375 expressed higher COX-2 levels than control cells (Fig. 6A). Moreover, we also measured the expression levels of microsomal Prostaglandin E synthase 1 (mPGES-1), the enzyme responsible of prostaglandin E2 synthesis and downstream to COX-2, and we observed that loss of KRIT1 promoted mPGES-1 upregulation (Fig. 6B), indicating that KRIT1 is able to regulate the inflammatory status in melanoma cells possibly contributing to melanoma malignancy.

4. DISCUSSION

In the present study we described for the first time evidences on the possible contribution of KRIT1 in melanoma progression. Even if most of the current literature links KRIT1 functions to endothelial cells and to cardiovascular development, KRIT1 is ubiquitously expressed. As previously reported, KRIT1 modulates endothelial cell functions by inducing proliferation, migration, angiogenesis and vascular permeability [22,55]. KRIT1 expression affects endothelial functions and its loss induces an endothelial phenotype highly invasive. It is well known that KRIT1 is an intracellular protein that interacts strongly and specifically with the tumor suppressor Rap1, [56] and it has been demonstrated that, in endothelial cells, KRIT1/Rap1 interaction regulates VE-cadherin/β-catenin association and KRIT1 loss increases the translocation of β-catenin to the nucleus [5,57]. In addition, Glading et al., showed that through this mechanism, KRIT1 mutations may lead to increased intestinal tumorigenesis [57]. Furthermore, Orso et al., have reported an anti-correlation between miR21 and KRIT1 that regulates epithelial tumor growth [27], supporting the idea that KRIT1 could play a role as tumor suppressor.

Cutaneous melanoma accounts for less than 5% of all skin cancer but it causes the majority of skin cancer deaths [58]. The main reason for the melanoma lethality is its high metastatic capacity even when the primary tumor is still significantly small in size. Intriguingly, we found that melanocytes constitutively express KRIT1, while in melanoma tissue, cancerous cells did not express KRIT1, or KRIT1 expression was limited to a focal immunopositivity. These findings support the idea that KRIT1 could be involved in melanoma progression and led us to explore the consequence of KRIT1 downregulation in A375 melanoma cell line. Our data indicate that KRIT1 deficiency increased cell survival, proliferation, migration and invasion, sustaining our original hypothesis.

Wnt/β□catenin signalling plays an important role in melanocyte biology, especially in the early stages of melanocyte transformation. β□catenin is an intracellular signal transducer of Wnt signalling and triggers transcription of genes involved in cell proliferation and invasion. Wnt/β□catenin signalling is frequently activated in melanoma and elevated β□catenin levels are positively correlated with melanoma aggressiveness. However, mechanisms that regulate β□catenin expression in melanoma are not fully understood. In our melanoma model, loss of KRIT1 induced increased β-catenin expression and its nuclear translocation, supporting the idea that KRIT1 could play a role as a tumor suppressor in melanoma. Additionally, since in epithelial cancers β□catenin controls the expression of proteins mainly involved in EMT, we explored the possibility that KRIT1 loss could induce the upregulation of mesenchymal markers that are associated to melanoma phenotype plasticity. Our data confirmed also this hypothesis being N-cadherin and vimentin upregulated after knocking down KRIT1.

Moreover, it is recognized that inflammatory process may drive melanoma cancer progression, and inhibition of COX-2 may inhibit melanoma metastasis [50,52,53]. In this work we showed that COX-2 and m-PGES1 are up-regulated after KRIT1 silencing in melanoma cells, supporting the idea that KRIT1 loss could increase melanoma aggressiveness also by modulating the inflammatory pathways.

5. CONCLUSIONS

In the present work, we have identified a novel pathway that could play a role in melanoma progression. Depletion of KRIT1 increased melanoma cells growth, migration and invasion, improved the β□catenin expression and its translocation into the nucleus, and induced the expression of markers of inflammation and melanoma plasticity.

Data deriving from the analysis of oncological databases, including canSAR Black (https://cansarblack.icr.ac.uk), COSMIC (https://cancer,sanger.ac.uk), and cBioPortal (https://www.cbioportal.org), showed an incidence of KRIT1 mutations in melanoma ranging between 3 and 12.5% versus a prevalence of 0% in benign melanocytic nevi, supporting our hypothesis that KRIT1 mutations play a role in melanoma development. Among the three mutated genes in the CCM disease, KRIT1 is by far the most involved in melanoma. Furthermore, data from the Cavernous Angioma patient registry (Angioma Alliance association, www.angioma.org) showed that the incidence of melanoma in CCM patients is about 1.2% versus an incidence of about 0.02% in general population (https://cancerstatisticscenter.cancer.org, https://seer.cancer.gov). Thus, even though specific information about the type of CCM gene (KRIT1/CCM1, CCM2 or CCM3) involved in CCM patients with melanoma is not available to date, the analysis of the different databases strongly suggest that patients bearing mutations in any of the three CCM genes are more likely to develop melanoma. The greater involvement of mutations of the KRIT1 gene in melanoma compared to the CCM2 and CCM3 genes, however, suggests that CCM patients bearing KRIT1 heterozygous mutations might be at higher risk of developing melanomas, possibly due to local effects in skin cells.

In conclusion, the data reported here strongly support the hypothesis that KRIT1 acts as a tumor suppressor in melanoma and its loss increases melanoma aggressiveness. Thank to this fundamental function, KRIT1 has the potentiality to be a future therapeutic target and diagnostic marker for melanoma.

Even though more in-depth epidemiological studies will be necessary to sustain and better elucidate these data, they will have important implications and relapses for both CCM and melanoma patients.

Acknowledgments

The authors are grateful to Giulia Macrì and Paola Nezi for providing help in some experiments, and Angioma Alliance for allowing access to the Cavernous Angioma patient registry.

Funding

This work was supported by the Telethon Foundation (grant GGP15219) to LT, MIUR (Progetto Dipartimento di Eccellenza 2018-2022) to LT, FF and JE, and FAR'19 to GV.

Figure legends

Figure 1. KRIT1 expression in melanoma and healthy tissues. (A) Strongly immunopositive melanocytes (as the one indicated by the arrow) in normal skin (a), and in a benign common nevus, BCN (b). Marked decrease in immunopositivity in a group of melanocytes of a dysplastic nevus, DN (c, arrow), and in a radial growth phase melanoma, RGPM (d). Almost completely immunonegative melanocytes in a vertical growth phase melanoma, VGPM (e) and in a melanoma metastasis, MelMet (f; the thick arrow points on an isolated immunopositive melanocyte, and the thin arrow on immunopositive vessels). Details of KRIT1 immunohistochemistry: normal skin (g); benign common nevus (h); dysplastic nevus (i); early growth phase melanoma (j); vertical growth phase melanoma (k), and melanoma metastases (l). The arrows in "k" and "l" boxes indicate immunopositive vessels. (B) Western blot analysis of KRIT1 levels in patient samples. The histogram represents the KRIT1 relative expression, normalized with β-actin expression (A.D.U.: arbitrary densitometry units) (** $p<0.01$; ***$p<0.001$; #$p<0.0001$). The scale bar in figures (a-f) represents 50 μm; in figures (g-l) represents 20 μm.

Figure 2. KRIT1 knockdown stimulates cellular proliferation in A375 cells (A). Western blot analysis of KRIT1 levels in siKRIT1 and siCTRL A375 cells. The histogram represents the relative expression, normalized with β-actin expression (A.D.U.: arbitrary densitometry units) (** $p<0.01$). (B) Cell viability of siKRIT1 and siCTRL A375 cells by MTT assays. These results are representative of three independent experiments (** $p<0.01$). (C) Cellular proliferation in siKRIT1 and siCTRL A375 cells. Images are obtained at 20X magnification. Results are reported as percentage of proliferating cells above the control (* $p<0.05$; ***$p<0.001$). (D) BrdU incorporation assay was performed in A375 cells transfected with either control siRNA (siCtrl) or KRIT1-targeting siRNA (siKRIT1) 24 hours post-transfection. Data shown are the averages of results from three independent experiments. *$p<0.05$. (E) Western blot analysis of cyclin D1 and p27 in siKRIT1 and siCTRL A375 cells. The histogram represents the relative expression, normalized to β-actin expression. (A.D.U.: arbitrary densitometry units) (* $p<0.05$, **$p<0.01$). The scale bar in figure above represents 400 μm.

Figure 3. KRIT1 downregulation increases migration and invasion in A375 melanoma cells. (A) Confluent monolayers of siKRIT1 and siCTRL A375 cells were scratched, and images were taken 6 and 12 hours post-wounding at 20x magnification. Data are reported as percentage of wound closed area for well and are representative of two independent experiments (*$p<0.05$). (B) Invasion assay. Image (20x magnification) of siKRIT1 and siCTRL A375 cells. Data are reported

as percentage of migrated cells for well and are representative of three independent experiments (*** $p<0.001$; # $p<0.0001$) (C) Enzymatic activity of MMP-2 in siKRIT1 and siCTRL A375 cells. Percentage of MMP-2 band was evaluated by quantitative densitometry and normalized to the number of cells/well (A.D.U.: arbitrary densitometry units). Data are representative of three independent experiments (# $p<0.001$). The scale bar in figures (A) and (B) represents 400 μm.

Figure 4. KRIT1 silencing induces β-catenin overexpression and nuclear translocation of A375 melanoma cells. (A) Western blot analysis of β-actin levels in siKRIT1 and siCTRL A375 cells. Quantification of β-catenin levels normalized to β-actin (A.D.U.: arbitrary densitometry units) (**$p<0.01$). (B) Immunofluorescence images of β-catenin (40X magnification) in siKRIT1 and siCTRL A375 cells. Quantification of nuclear and cytoplasmatic β-catenin fluorescence intensity (CTCF: corrected total cell fluorescence) # $p<0.001$). The scale bar in figures above represents 15 μm.

Figure 5. KRIT1 silencing induces epithelial mesenchymal transition of A375 melanoma cells. (A) Western blot analysis of vimentin and N-cadherin expression in siKRIT1 and siCTRL A375 cells. Quantification of vimentin and N-cadherin levels normalized to β-actin (A.D.U.:arbitrary densitometry units) (*$p<0.05$; ***$p<0.001$). (B) Immunofluorescence images of vimentin and N-cadherin (40X magnification) in siKRIT1 and siCTRL A375 cells. Quantification of N-cadherin and vimentin fluorescence intensity (CTCF: corrected total cell fluorescence) (* $p<0.05$; ** $p<0.01$). The scale bar in figures above represents 15 μm.

Figure 6. KRIT1 silencing induces COX-2 and mPGES-1 expression. (A, B) Western blot analysis of COX-2 and, mPGES-1 expression in siKRIT1 and siCTRL A375 cells. Quantification of COX-2 and mPGES-1 levels normalized to β-actin (A.D.U.: arbitrary densitometry units) (**$p<0.01$).

BIBLIOGRAPHY:

[1] I. Serebriiskii, J. Estojak, G. Sonoda, J.R. Testa, E.A. Golemis, Association of Krev-1/rap1a with Krit1, a novel ankyrin repeat-containing protein encoded by a gene mapping to 7q21-22, Oncogene. 15 (1997) 1043–1049. doi:10.1038/sj.onc.1201268.

[2] P. Guazzi, L. Goitre, E. Ferro, V. Cutano, C. Martino, L. Trabalzini, S.F. Retta, Identification of the Kelch Family Protein Nd1-L as a Novel Molecular Interactor of KRIT1, PLoS One. 7 (2012) e44705. doi:10.1371/journal.pone.0044705.

[3] J.S. Zawistowski, I.G. Serebriiskii, M.F. Lee, E.A. Golemis, D.A. Marchuk, KRIT1 association with the integrin-binding protein ICAP-1: a new direction in the elucidation of cerebral cavernous malformations (CCM1) pathogenesis, Hum. Mol. Genet. 11 (2002) 389–396. doi:10.1093/hmg/11.4.389.

[4] J.S. Zawistowski, L. Stalheim, M.T. Uhlik, A.N. Abell, B.B. Ancrile, G.L. Johnson, D.A. Marchuk, CCM1 and CCM2 protein interactions in cell signaling: implications for cerebral cavernous malformations pathogenesis, Hum. Mol. Genet. 14 (2005) 2521–2531. doi:10.1093/hmg/ddi256.

[5] A. Glading, J. Han, R.A. Stockton, M.H. Ginsberg, KRIT-1/CCM1 is a Rap1 effector that regulates endothelial cell–cell junctions, J. Cell Biol. 179 (2007) 247–254. doi:10.1083/jcb.200705175.

[6] E. Faurobert, C. Albiges-Rizo, Recent insights into cerebral cavernous malformations: a complex jigsaw puzzle under construction., FEBS J. 277 (2010) 1084–96. doi:10.1111/j.1742-4658.2009.07537.x.

[7] C. Denier, J.M. Gasc, F. Chapon, V. Domenga, C. Lescoat, A. Joutel, E. Tournier-Lasserve, Krit1/cerebral cavernous malformation 1 mRNA is preferentially expressed in neurons and epithelial cells in embryo and adult, Mech. Dev. (2002). doi:10.1016/S0925-4773(02)00209-5.

[8] T. Sahoo, E.W. Johnson, J.W. Thomas, P.M. Kuehl, T.L. Jones, C.G. Dokken, J.W. Touchman, C.J. Gallione, S.Q. Lee-Lin, B. Kosofsky, J.H. Kurth, D.N. Louis, G. Mettler, L. Morrison, A. Gil-Nagel, S.S. Rich, J.M. Zabramski, M.S. Boguski, E.D. Green, D.A. Marchuk, Mutations in the gene encoding KRIT1, a Krev-1/rap1a binding protein, cause cerebral cavernous malformations (CCM1), Hum. Mol. Genet. 8 (1999) 2325–2333. doi:10.1093/hmg/8.12.2325.

[9] S.L. Couteulx, H.H. Jung, P. Labauge, J. Houtteville, C. Lescoat, M. Cecillon, E. Marechal, A. Joutel, J. Bach, E. Tournier-lasserve, Cause Hereditary Cavernous Angiomas, Nat. Genet. (1999). doi:10.1038/13815.

[10] S. Batra, D. Lin, P.F. Recinos, J. Zhang, D. Rigamonti, Cavernous malformations: natural history, diagnosis and treatment, Nat. Rev. Neurol. 5 (2009) 659–670. doi:10.1038/nrneurol.2009.177.

[11] J. Gault, H. Sarin, N.A. Awadallah, R. Shenkar, I.A. Awad, Pathobiology of human cerebrovascular malformations: basic mechanisms and clinical relevance., Neurosurgery. 55 (2004) 1–16; discussion 16-7. http://www.ncbi.nlm.nih.gov/pubmed/15214969 (accessed September 3, 2019).

[12] D. Rigamonti, Cavernous malformations of the nervous system, 2011. doi:10.1017/CBO9781139003636.

[13] A. Padarti, J. Zhang, Recent advances in cerebral cavernous malformation research., Vessel Plus. 2 (2018) 21. doi:10.20517/2574-1209.2018.34.

[14] Y. Wang, Y. Li, J. Zou, S.P. Polster, R. Lightle, T. Moore, M. Dimaano, T.C. He, C.R. Weber, I.A. Awad, L. Shen, The cerebral cavernous malformation disease causing gene KRIT1 participates in intestinal epithelial barrier maintenance and regulation, FASEB J. (2019). doi:10.1096/fj.201800343R.

[15] F. Finetti, I. Schiavo, J. Ercoli, A. Zotta, E. Boda, S.F. Retta, L. Trabalzini, KRIT1 loss-mediated upregulation of NOX1 in stromal cells promotes paracrine pro-angiogenic responses, Cell. Signal. 68 (2020) 109527. doi:10.1016/j.cellsig.2020.109527.

[16] C. Antognelli, E. Trapani, S. Delle Monache, A. Perrelli, M. Daga, S. Pizzimenti, G. Barrera, P. Cassoni, A. Angelucci, L. Trabalzini, V.N. Talesa, L. Goitre, S.F. Retta, KRIT1 loss-of-function induces a chronic Nrf2-mediated adaptive homeostasis that sensitizes cells to oxidative stress: Implication for Cerebral Cavernous Malformation disease, Free Radic. Biol. Med. (2018). doi:10.1016/j.freeradbiomed.2017.11.014.

[17] L. Goitre, P. V. DiStefano, A. Moglia, N. Nobiletti, E. Baldini, L. Trabalzini, J. Keubel, E. Trapani, V. V. Shuvaev, V.R. Muzykantov, I.H. Sarelius, S.F. Retta, A.J. Glading, Up-regulation of NADPH oxidase-mediated redox signaling contributes to the loss of barrier function in KRIT1 deficient endothelium, Sci. Rep. 7 (2017) 8296. doi:10.1038/s41598-017-08373-4.

[18] L. Goitre, E. De Luca, S. Braggion, E. Trapani, M. Guglielmotto, F. Biasi, M. Forni, A. Moglia, L. Trabalzini, S.F. Retta, KRIT1 loss of function causes a ROS-dependent upregulation of c-Jun, Free Radic. Biol. Med. (2014). doi:10.1016/j.freeradbiomed.2013.11.020.

[19] A.J. Glading, F. Finetti, L. Trabalzini, Disease models in cerebral cavernous malformations, Drug Discov. Today Dis. Model. xxx (2019) 1–9. doi:10.1016/j.ddmod.2019.10.009.

[20] F. Francalanci, M. Avolio, E. De Luca, D. Longo, V. Menchise, P. Guazzi, F. Sgrò, M. Marino, L. Goitre, F. Balzac, L. Trabalzini, S.F. Retta, Structural and functional differences between KRIT1A and KRIT1B isoforms: A framework for understanding CCM pathogenesis, Exp. Cell Res. 315 (2009) 285–303. doi:10.1016/j.yexcr.2008.10.006.

[21] L. Maddaluno, N. Rudini, R. Cuttano, L. Bravi, C. Giampietro, M. Corada, L. Ferrarini, F. Orsenigo, E. Papa, G. Boulday, E. Tournier-Lasserve, F. Chapon, C. Richichi, S.F. Retta, M.G. Lampugnani, E. Dejana, EndMT contributes to the onset and progression of cerebral cavernous malformations, Nature. 498 (2013) 492–496. doi:10.1038/nature12207.

[22] M.G. Lampugnani, F. Orsenigo, N. Rudini, L. Maddaluno, G. Boulday, F. Chapon, E. Dejana, CCM1 regulates vascular-lumen organization by inducing endothelial polarity, J. Cell Sci. (2010). doi:10.1242/jcs.059329.

[23] J. Wüstehube, A. Bartol, S.S. Liebler, R. Brütsch, Y. Zhu, U. Felbor, U. Sure, H.G. Augustin, A. Fischer, Cerebral cavernous malformation protein CCM1 inhibits sprouting angiogenesis by activating DELTA-NOTCH signaling, Proc. Natl. Acad. Sci. 107 (2010) 12640–12645. doi:10.1073/pnas.1000132107.

[24] P. V. DiStefano, J.M. Kuebel, I.H. Sarelius, A.J. Glading, KRIT1 Protein Depletion Modifies Endothelial Cell Behavior via Increased Vascular Endothelial Growth Factor (VEGF) Signaling, J. Biol. Chem. 289 (2014) 33054–33065. doi:10.1074/jbc.M114.582304.

[25] L. Goitre, F. Balzac, S. Degani, P. Degan, S. Marchi, P. Pinton, S.F. Retta, KRIT1 regulates the homeostasis of intracellular reactive oxygen species, PLoS One. (2010). doi:10.1371/journal.pone.0011786.

[26] F. Vieceli Dalla Sega, R. Mastrocola, G. Aquila, F. Fortini, C. Fornelli, A. Zotta, A.S. Cento, A. Perrelli, E. Boda, A. Pannuti, S. Marchi, P. Pinton, R. Ferrari, P. Rizzo, S.F. Retta, KRIT1 Deficiency Promotes Aortic Endothelial Dysfunction., Int. J. Mol. Sci. 20 (2019). doi:10.3390/ijms20194930.

[27] F. Orso, F. Balzac, M. Marino, A. Lembo, S.F. Retta, D. Taverna, MiR-21 coordinates tumor growth and modulates KRIT1 levels, Biochem. Biophys. Res. Commun. 438 (2013) 90–96. doi:10.1016/j.bbrc.2013.07.031.

[28] J. Abou-Fadel, Y. Qu, E.M. Gonzalez, M. Smith, J. Zhang, Emerging roles of CCM genes during tumorigenesis with potential application as novel biomarkers across major types of cancers, Oncol. Rep. 43 (2020) 1945–1963. doi:10.3892/or.2020.7550.

[29] E. Erdei, S.M. Torres, A new understanding in the epidemiology of melanoma, Expert Rev. Anticancer Ther. (2010). doi:10.1586/era.10.170.

[30] Z. Kutlubay, B. Engin, S. Serdaroglu, Y. Tuzu, Current Management of Malignant Melanoma: State of the Art, in: Highlights Ski. Cancer, 2013. doi:10.5772/55304.

[31] M. Rastrelli, S. Tropea, C. Rossi, M. Alaibac, Melanoma Risk Factors, In Vivo. (2012).

[32] V.C. Gorantla, J.M. Kirkwood, State of Melanoma. An Historic Overview of a Field in Transition, Hematol. Oncol. Clin. North Am. (2014). doi:10.1016/j.hoc.2014.02.010.

[33] A. Sandru, S. Voinea, E. Panaitescu, A. Blidaru, Survival rates of patients with metastatic malignant melanoma, J. Med. Life. (2014).

[34] N. Klebanov, W.M. Lin, M. Artomov, M. Shaughnessy, C.N. Njauw, R. Bloom, A.K. Eterovic, K. Chen, T.B. Kim, S.S. Tsao, H. Tsao, Use of Targeted Next-Generation Sequencing to Identify Activating Hot Spot Mutations in Cherry Angiomas, JAMA Dermatology. 155 (2019) 211–215. doi:10.1001/jamadermatol.2018.4231.

[35] A.J. Parish, V. Nguyen, A.M. Goodman, K. Murugesan, G.M. Frampton, R. Kurzrock, GNAS, GNAQ, and GNA11 alterations in patients with diverse cancers, Cancer. 124 (2018) 4080–4089. doi:10.1002/cncr.31724.

[36] C. Cavicchio, M. Benedusi, E. Pambianchi, A. Pecorelli, F. Cervellati, V. Savelli, D. Calamandrei, E. Maellaro, G. Rispoli, E. Maioli, G. Valacchi, Potassium Ascorbate with Ribose: Promising Therapeutic Approach for Melanoma Treatment, Oxid. Med. Cell. Longev. 2017 (2017). doi:10.1155/2017/4256519.

[37] F. Ferrara, E. Pambianchi, A. Pecorelli, B. Woodby, N. Messano, J.P. Therrien, M.A. Lila, G. Valacchi, Redox regulation of cutaneous inflammasome by ozone exposure, Free Radic. Biol. Med. (2019) 0–1. doi:10.1016/j.freeradbiomed.2019.11.031.

[38] X.M. Muresan, M.S. Narzt, B. Woodby, F. Ferrara, F. Gruber, G. Valacchi, Involvement of cutaneous SR-B1 in skin lipid homeostasis, Arch. Biochem. Biophys. (2019). doi:10.1016/j.abb.2019.03.005.

[39] A. Fallacara, S. Vertuani, G. Panozzo, A. Pecorelli, G. Valacchi, S. Manfredini, Novel artificial tears containing cross-linked hyaluronic acid: An in vitro re-epithelialization study, Molecules. 22 (2017) 1–13. doi:10.3390/molecules22122104.

[40] F. Finetti, E. Terzuoli, E. Bocci, I. Coletta, L. Polenzani, G. Mangano, M.A. Alisi, N. Cazzolla, A. Giachetti, M. Ziche, S. Donnini, Pharmacological inhibition of microsomal prostaglandin E synthase-1 suppresses epidermal growth factor receptor-mediated tumor growth and angiogenesis, PLoS One. 7 (2012). doi:10.1371/journal.pone.0040576.

[41] I. Crivellari, C. Sticozzi, G. Belmonte, X.M. Muresan, F. Cervellati, A. Pecorelli, C. Cavicchio, E. Maioli, C.C. Zouboulis, M. Benedusi, C. Cervellati, G. Valacchi, SRB1 as a new redox target of cigarette smoke in human sebocytes, Free Radic. Biol. Med. 102 (2017)

47–56. doi:10.1016/j.freeradbiomed.2016.11.021.

[42] F. Finetti, R. Solito, L. Morbidelli, A. Giachetti, M. Ziche, S. Donnini, Prostaglandin E2 regulates angiogenesis via activation of fibroblast growth factor receptor-1, J. Biol. Chem. 283 (2008) 2139–2146. doi:10.1074/jbc.M703090200.

[43] G. Allavena, B. Del Bello, P. Tini, N. Volpi, G. Valacchi, C. Miracco, L. Pirtoli, E. Maellaro, Trehalose inhibits cell proliferation and amplifies long-term temozolomide- and radiation-induced cytotoxicity in melanoma cells: A role for autophagy and premature senescence, J. Cell. Physiol. 234 (2019) 11708–11721. doi:10.1002/jcp.27838.

[44] O. Guzeloglu-Kayisli, U.A. Kayisli, N.M. Amankulor, J.R. Voorhees, O. Gokce, M.L. DiLuna, M.S.H. Laurans, G. Luleci, M. Gunel, Krev1 Interaction Trapped-1/Cerebral Cavernous Malformation-1 protein expression during early angiogenesis, J. Neurosurg. 100 (2004) 481–487. doi:10.3171/ped.2004.100.5.0481.

[45] E.S. Radisky, D.C. Radisky, Matrix metalloproteinase-induced epithelial-mesenchymal transition in breast cancer, J. Mammary Gland Biol. Neoplasia. (2010). doi:10.1007/s10911-010-9177-x.

[46] T. Reya, H. Clevers, Wnt signalling in stem cells and cancer. 434, 843–850 (2005)., 2005.

[47] K. Prabhakar, C.I. Rodríguez, A.S. Jayanthy, D.M. Mikheil, A.I. Bhasker, R.J. Perera, V. Setaluri, Role of miR-214 in regulation of β-catenin and the malignant phenotype of melanoma, Mol. Carcinog. (2019). doi:10.1002/mc.23089.

[48] K.M. Cadigan, Wnt-β-catenin signaling, Curr. Biol. (2008). doi:10.1016/j.cub.2008.08.017.

[49] C.Y. Liu, H.H. Lin, M.J. Tang, Y.K. Wang, Vimentin contributes to epithelial-mesenchymal transition ancer cell mechanics by mediating cytoskeletal organization and focal adhesion maturation, Oncotarget. (2015). doi:10.18632/oncotarget.3862.

[50] K.M. Kim, A.R. Im, S.H. Kim, J.W. Hyun, S. Chae, Timosaponin AIII inhibits melanoma cell migration by suppressing COX-2 and in vivo tumor metastasis, Cancer Sci. 107 (2016) 181–188. doi:10.1111/cas.12852.

[51] A.-C. Goulet, J.G. Einsphar, D.S. Alberts, A. Beas, C. Burk, A. Bhattacharyya, J. Bangert, J.M. Harmon, H. Fujiwara, A. Koki, M.A. Nelson, Analysis of cyclooxygenase 2 (COX-2) expression during malignant melanoma progression., Cancer Biol. Ther. 2 (n.d.) 713–8. http://www.ncbi.nlm.nih.gov/pubmed/14688483 (accessed January 30, 2020).

[52] E. Panza, P. De Cicco, G. Ercolano, C. Armogida, G. Scognamiglio, A.M. Anniciello, G. Botti, G. Cirino, A. Ianaro, Differential expression of cyclooxygenase-2 in metastatic melanoma affects progression free survival, Oncotarget. 7 (2016) 57077–57085. doi:10.18632/oncotarget.10976.

[53] P. Zhou, J. Qin, Y. Li, G. Li, Y. Wang, N. Zhang, P. Chen, C. Li, Combination therapy of PKCζ and COX-2 inhibitors synergistically suppress melanoma metastasis, J. Exp. Clin. Cancer Res. 36 (2017) 1–12. doi:10.1186/s13046-017-0585-2.

[54] N. Hashemi Goradel, M. Najafi, E. Salehi, B. Farhood, K. Mortezaee, Cyclooxygenase-2 in cancer: A review, J. Cell. Physiol. 234 (2019) 5683–5699. doi:10.1002/jcp.27411.

[55] S.F. Retta, A.J. Glading, Oxidative stress and inflammation in cerebral cavernous malformation disease pathogenesis: Two sides of the same coin, Int. J. Biochem. Cell Biol. (2016). doi:10.1016/j.biocel.2016.09.011.

[56] X. Li, R. Zhang, K.M. Draheim, W. Liu, D.A. Calderwood, T.J. Boggon, Structural basis for small G protein effector interaction of ras-related protein 1 (Rap1) and adaptor protein krev interaction trapped 1 (KRIT1), J. Biol. Chem. 287 (2012) 22317–22327. doi:10.1074/jbc.M112.361295.

[57] A.J. Glading, M.H. Ginsberg, Rap1 and its effector KRIT1/CCM1 regulate -catenin signaling, Dis. Model. Mech. 3 (2010) 73–83. doi:10.1242/dmm.003293.

[58] M. Potrony, C. Badenas, P. Aguilera, J.A. Puig-Butille, C. Carrera, J. Malvehy, S. Puig, Update in genetic susceptibility in melanoma, Ann. Transl. Med. 3 (2015). doi:10.3978/j.issn.2305-5839.2015.08.11.

Table 1: Main clinicopathological data of melanocytic lesions used in this study
A): BCN, benign common nevi; DN, dysplastic nevi
B): RGPM, radial growth phase melanomas; VGPM, vertical growth phase melanomas; MelMet, melanoma metastases; MM, malignant melanomas

A)

	BCN	DN
(n)	5	5
Male/female	3/2	5/0
Median age (range)	40 (29-55)	45(41-64)
Site (HN/T/L/F)	1/3/1/0	0/5/0/0
AML (BCN/DN/MM/No)	3/0/0/2	0/4/2/0*

B)

	RGPM	VGPM	MEL MET
(n)	5	23	11
Male/female	2/3	10/13	3/8
Median age (range)	72 (44-87)	67 (33-86)	59 (25-86)
MM Site (HN/T/L)	2/2/1/0	7/7/9	-
MelMet Site (S/LN/V)	-	-	4/4/3
MM type (ALM/LMM/NM/NeM/SSM)	0/2/0/0/3	1/3/6//1/12	-
pT (is/1a/1b/2/3/4)	3/2/0/0/0/0	0/2/0/8/7/6	-
CSDS/non-CSDS	3/2	4/19	-
M(n)/wt(n)/nd(n):			
BRAF	wt (1)/nd (4)	p.V600E3(14)/wt(3)	p.V600E(3)/p.V600K(1) p.G466(1)/wt(6)
NRAS	wt(1) /nd (4)	p.Q61R(3);p.Q61K(2)/wt (18)	p.Q61R(1)/wt (10)
C-KIT	wt(1)/nd (4)	p.L576P(1)/wt(22)	wt(11)
Progression (Smet/LNmet/NoP)	0/0/5	8/7/8	-
Status(A/D/U)	5/0/0	17/6/0	7/3/1

HN, head and neck; T, trunk; L, limbs; F, foot; AML, associated melanocytic lesions (BCN, benign common nevi, DN, dysplastic nevi; MM, malignant melanomas; No, none)
(n), number of cases
* a patient with Dysplastic nevus syndrome had both DN and MM
HN, head and neck; T, trunk; L, limbs
S, skin; LN, lymph node; V, visceral
ALM, acral lentiginous melanoma; LMM, lentigo maligna melanoma; NM, nodular melanoma; NeM, nevoid melanoma; SSM, superficial spreading melanoma
pT according to AJCCC, 8th ed.
CSDs, chronically sun damaged skin; non-CSDs, not chronically sun damaged skin
M, mutation; wt, wild type; nd, not done
Smet, skin metastases; LNmet, lymph node metastases; NoP, not progressed; U, unknown
A, alive; D, dead; U, unknown

Figure 1

A

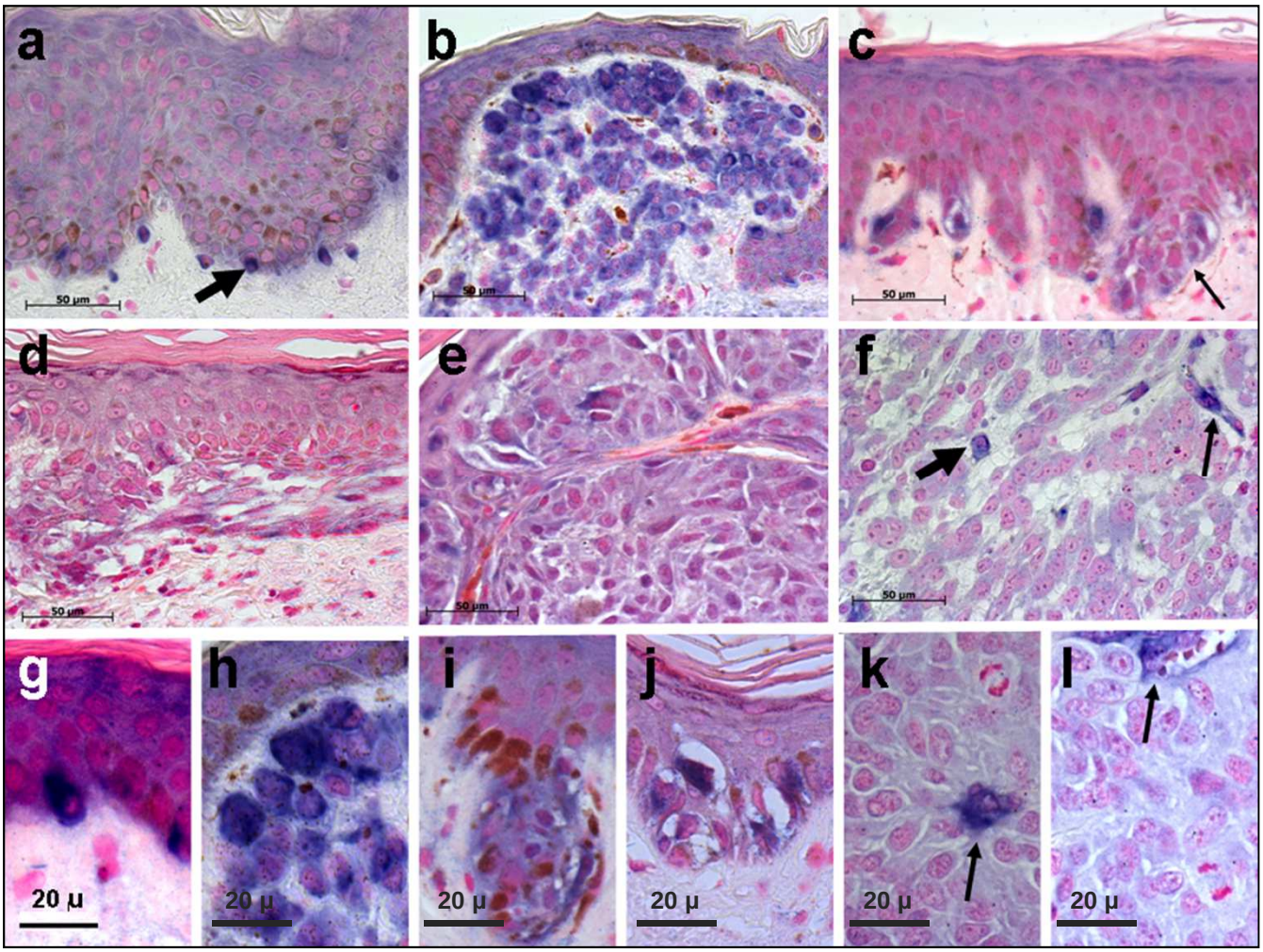
a
b
c
d
e
f
g
h
i
j
k
l
50 µm
20 µ

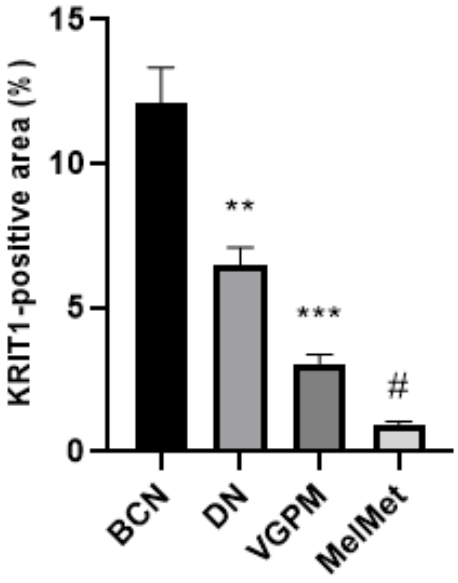
KRIT1-positive area (%)
15
10
5
0
**
***
#
BCN
DN
VGPM
MelMet

Figure 1

B

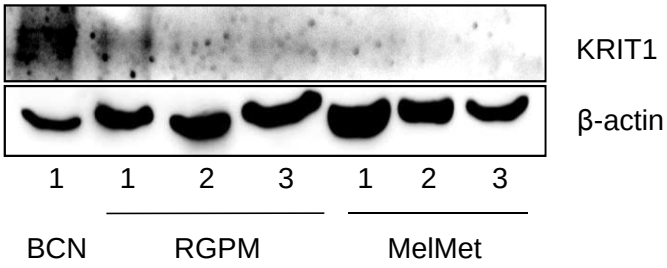
KRIT1
β-actin
1 1 2 3 1 2 3
BCN
RGPM
MelMet

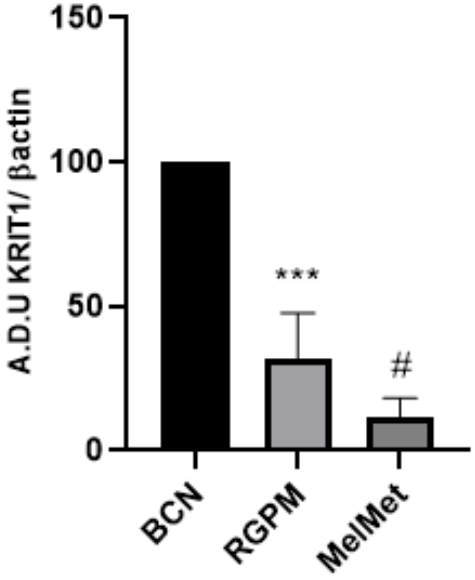
A.D.U KRIT1/ βactin
150
100
50
0
***
#
BCN
RGPM
MelMet

Figure 2

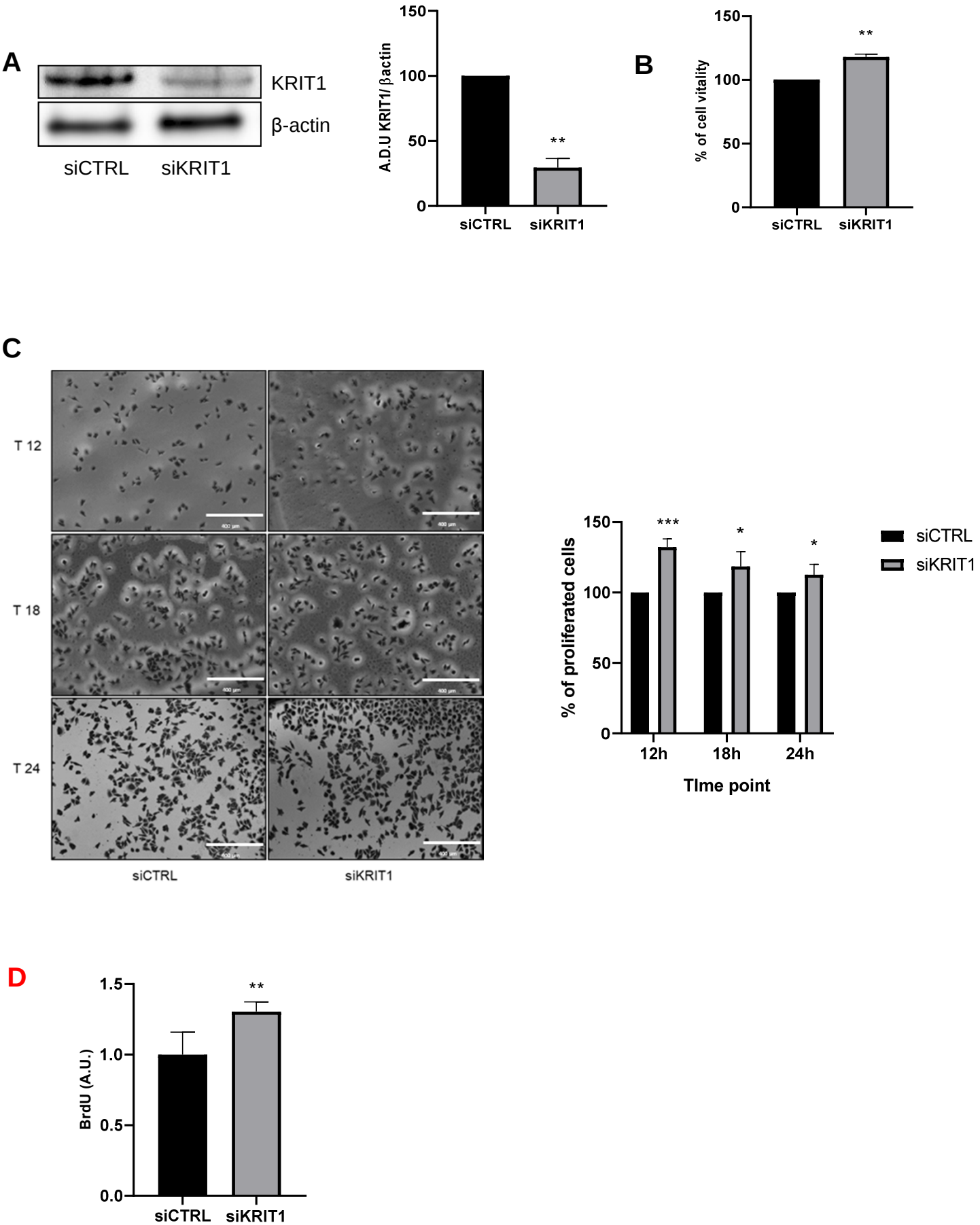
A
KRIT1
β-actin
siCTRL
siKRIT1
A.D.U KRIT1/ βactin
150
100
50
0
**
siCTRL
siKRIT1
B
% of cell vitality
150
100
50
0
**
siCTRL
siKRIT1
C
T 12
T 18
T 24
siCTRL
siKRIT1
% of proliferated cells
150
100
50
0
***
*
*
12h
18h
24h
TIme point
siCTRL
siKRIT1
D
BrdU (A.U.)
1.5
1.0
0.5
0.0
**
siCTRL
siKRIT1

E

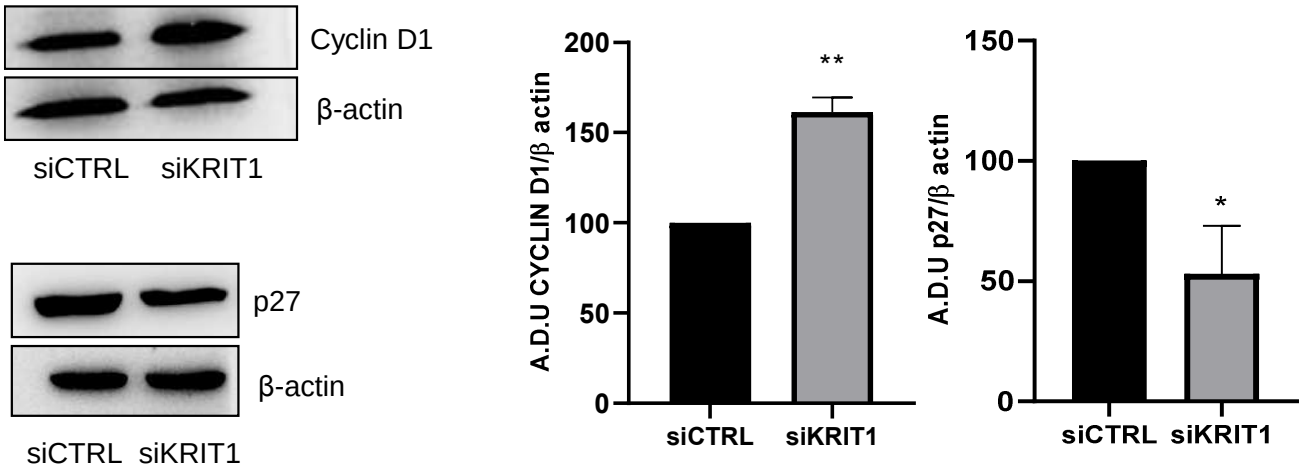
Cyclin D1
β-actin
siCTRL siKRIT1
p27
β-actin
siCTRL siKRIT1
A.D.U CYCLIN D1/β actin
200
150
100
50
0
**
siCTRL siKRIT1
A.D.U p27/β actin
150
100
50
0
*
siCTRL siKRIT1

Figure 3

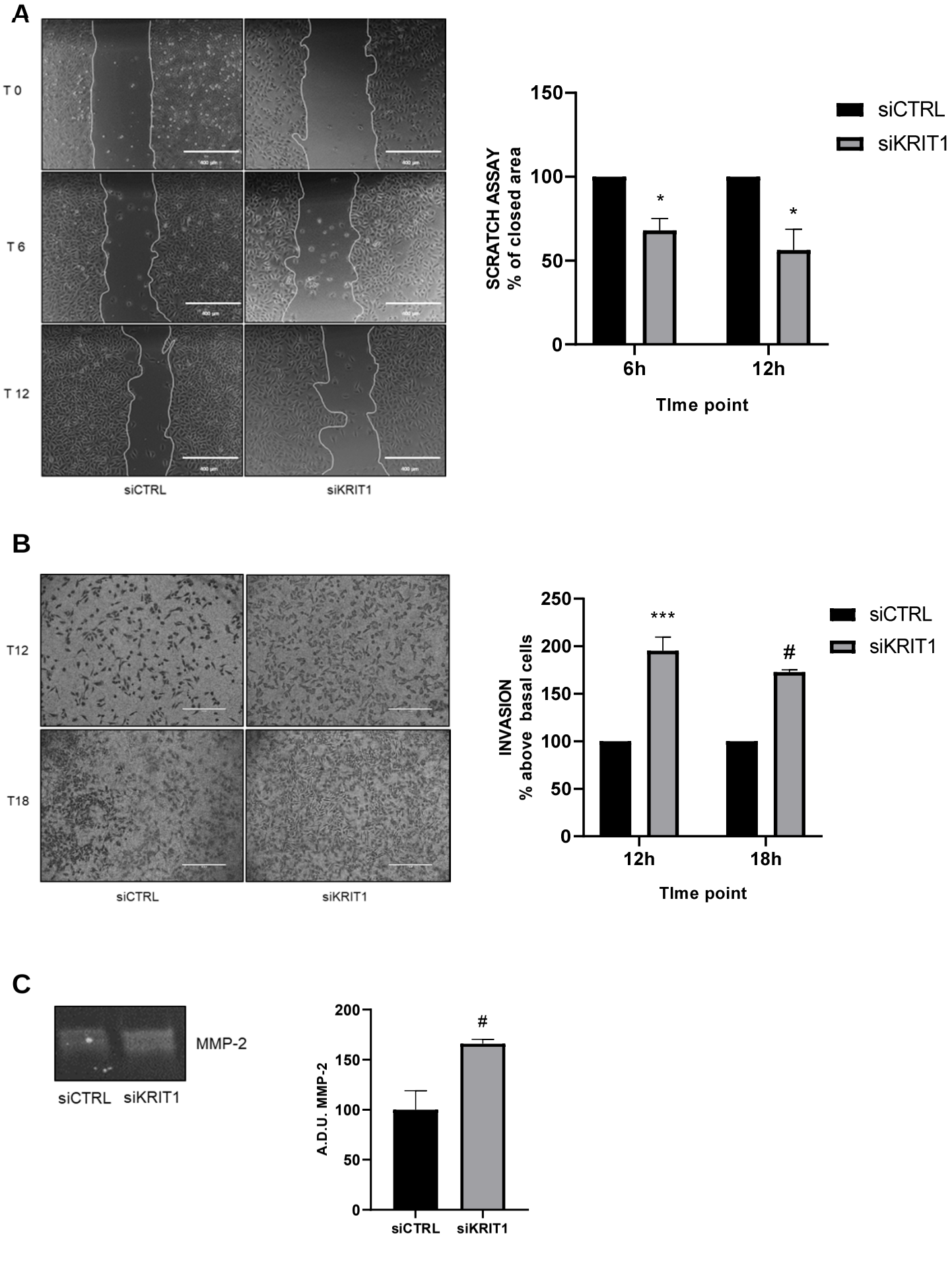
A
T 0
T 6
T 12
siCTRL
siKRIT1
SCRATCH ASSAY
% of closed area
150
100
50
0
*
*
6h
12h
TIme point
siCTRL
siKRIT1
B
T12
T18
siCTRL
siKRIT1
INVASION
% above basal cells
250
200
150
100
50
0
***
#
12h
18h
TIme point
siCTRL
siKRIT1
C
MMP-2
siCTRL siKRIT1
A.D.U. MMP-2
200
150
100
50
0
#
siCTRL
siKRIT1

Figure 4

A


β-catenin
β-actin
siCTRL siKRIT1

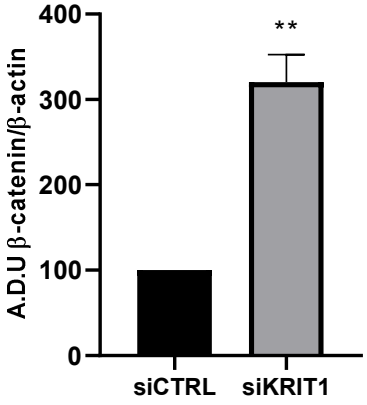
400
300
200
100
0
**
A.D.U β-catenin/β-actin
siCTRL
siKRIT1

B

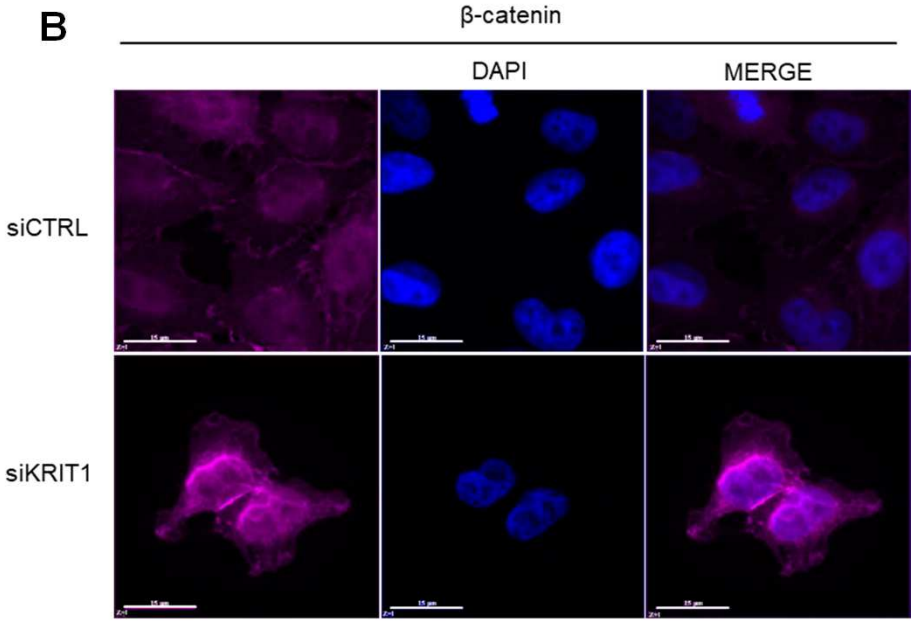
β-catenin
DAPI
MERGE
siCTRL
siKRIT1

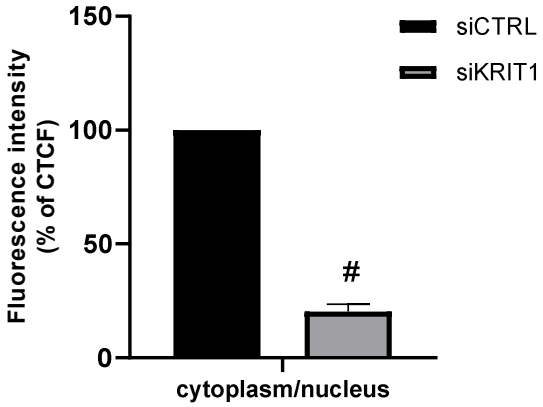
150
100
50
0
Fluorescence intensity
(% of CTCF)
#
cytoplasm/nucleus
siCTRL
siKRIT1

Figure 5

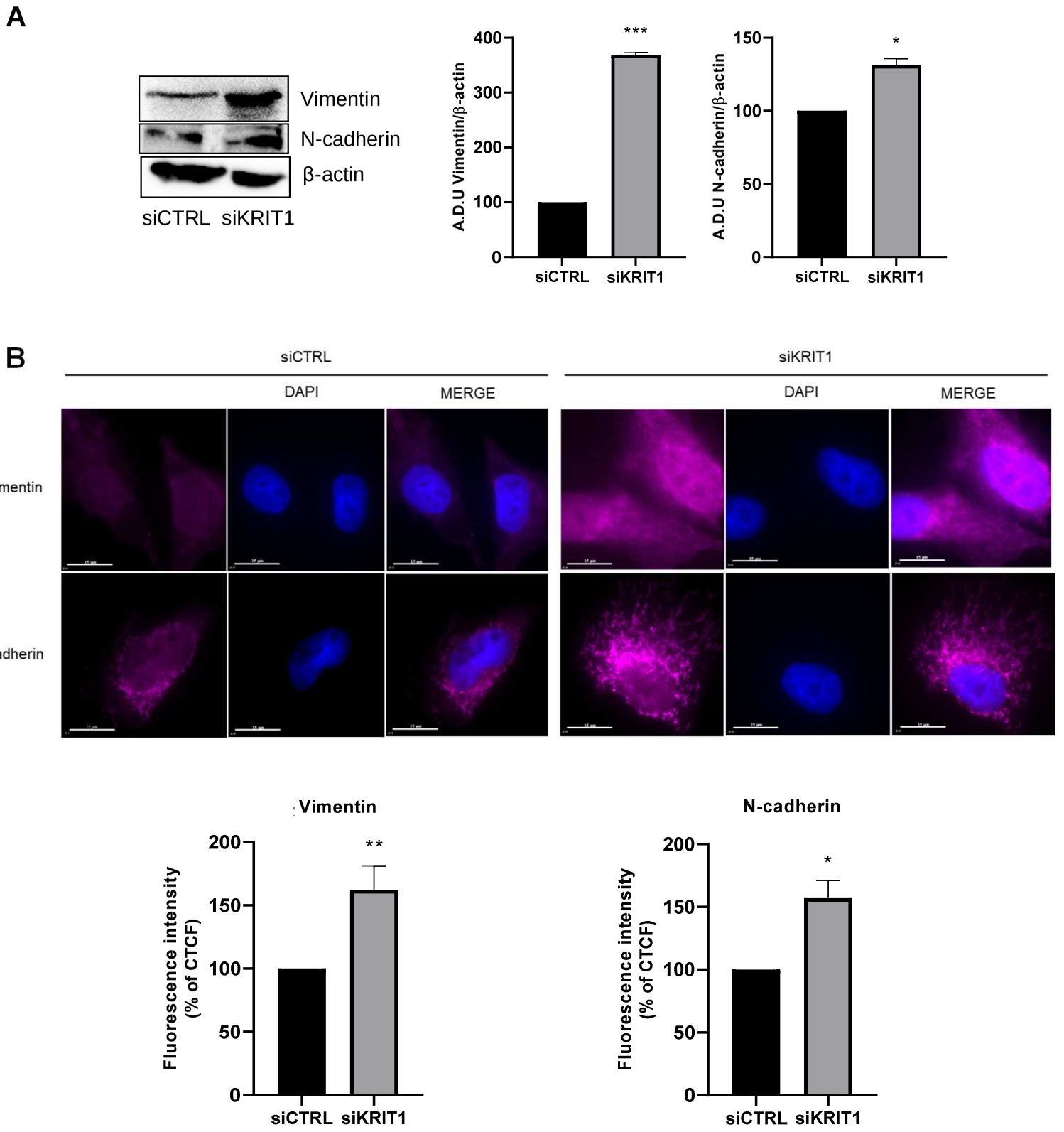
A
Vimentin
N-cadherin
β-actin
siCTRL siKRIT1
A.D.U Vimentin/β-actin
400
300
200
100
0
***
siCTRL siKRIT1
A.D.U N-cadherin/β-actin
150
100
50
0
*
siCTRL siKRIT1
B
siCTRL
siKRIT1
DAPI
MERGE
DAPI
MERGE
Vimentin
N-cadherin
Vimentin
Fluorescence intensity (% of CTCF)
200
150
100
50
0
**
siCTRL siKRIT1
N-cadherin
Fluorescence intensity (% of CTCF)
200
150
100
50
0
*
siCTRL siKRIT1

Figure 6

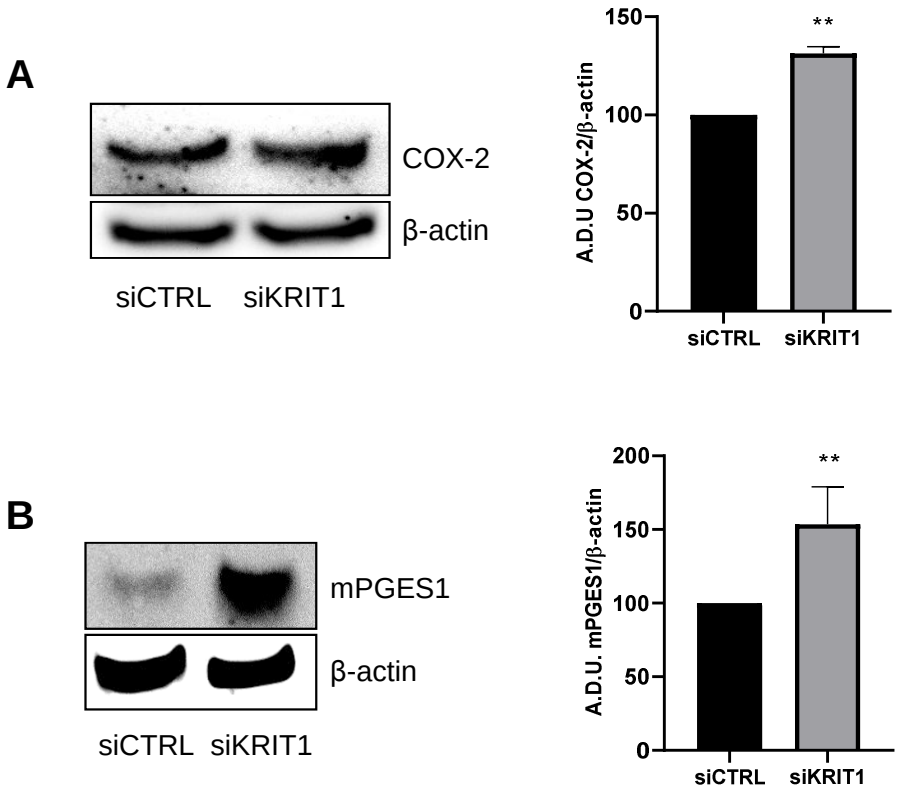
A
COX-2
β-actin
siCTRL
siKRIT1
A.D.U COX-2/β-actin
150
100
50
0
**
siCTRL
siKRIT1
B
mPGES1
β-actin
siCTRL
siKRIT1
A.D.U. mPGES1/β-actin
200
150
100
50
0
**
siCTRL
siKRIT1